THE ASTROPHYSICAL JOURNAL, 521:L29–L32, 1999 August 10

86, 43, AND 22 GHz VLBI OBSERVATIONS OF 3C 120

JOSÉ-LUIS GÓMEZ
Instituto de Astrofísica de Andalucía, Consejo Superior de Investigaciones Científicas,
Apartado 3004, 18080 Granada, Spain; jlgomez@iaa.es
ALAN P. MARSCHER
Department of Astronomy, Boston University, 725 Commonwealth Avenue,
Boston, MA 02215; marscher@bu.edu
AND
ANTONIO ALBERDI
Instituto de Astrofísica de Andalucía, Consejo Superior de Investigaciones Científicas,
Apartado 3004, 18080 Granada, Spain; antxon@iaa.es
Received 1999 March 31; accepted 1999 June 8; published 1999 July 6

ABSTRACT

We present the first 86 GHz VLBI observations of the radio galaxy 3C 120, together with contemporaneous 43 and 22 GHz polarimetric VLBA observations. The very high angular resolution obtained at 86 GHz provides an upper limit to the size of the core of 54 μas (0.025 h^{-1} pc). This represents a direct determination of the base of the jet that is independent of variability arguments (which depend on uncertain estimates of the Doppler factor) and places it below approximately 1 lt-month. Comparison with previous VLBA observations after a 1 yr interval shows pronounced changes in the structure and polarization of the jet. Most of the components are found to follow a curved path while undergoing a steepening of their spectra accompanied by a decrease in total and polarized emission. However, at least one component is observed to follow a quasi-ballistic motion, accompanied by a flattening of its spectrum as well as an increase in total and polarized flux. This may be explained by its interaction with the external medium, resulting in a shock that enhances the emission and aligns the magnetic field perpendicular to the component motion, thereby producing an increase of the degree of polarization from undetected values to as high as 15%. A second strong component, with the highest degree of polarization (23%), is found to have experienced a displacement from the ridge line of the structural position angle of the jet as it moved downstream. We have found a mean swing to the south of the position angle of the innermost components of ~6° between late 1996 and 1997, which may be responsible for the jet curvature observed at parsec and kiloparsec scales.

Subject headings: galaxies: active — galaxies: individual (3C 120) — galaxies: jets — polarization — radio continuum: galaxies

1. INTRODUCTION

The radio galaxy 3C 120 is a powerful and variable emitter of radiation at all observing frequencies. It is usually classified as a Seyfert 1 galaxy (Burbidge 1967), although its optical morphology is also consistent with that of a broad-line radio galaxy. It was among the first sources in which superluminal motion was detected, on a scale of parsecs (Seielstad et al. 1979; Walker, Benson, & Unwin 1987) to tens of parsecs (Benson et al. 1988; Walker 1997). An optical counterpart of the radio jet has also been detected (Hjorth et al. 1995). The radio galaxy 3C 120 is among the closest known extragalactic superluminal sources ($z = 0.033$), allowing the study of its inner jet structure with unusually fine linear resolution for this class of objects. Previous observations using NRAO's[1] Very Long Baseline Array (VLBA) at 22 and 43 GHz (Gómez et al. 1998, hereafter G98) revealed a very rich inner jet structure containing up to 10 different superluminal components, with velocities between 2.3 and 5.5 $h^{-1}c$, mapped with a linear resolution of 0.07 h^{-1} pc. Linear polarization was also detected in several components, revealing a magnetic field orientation that varies with respect to the jet flow direction as a function of frequency, epoch, and position along the jet.

In this Letter, we present the first 86 GHz Coordinated Millimeter VLBI Array (CMVA) observations of 3C 120, providing an angular resolution of 54 μas, which for this source represents a linear resolution of 0.025 h^{-1} pc. We also present contemporaneous 22 and 43 GHz polarimetric VLBA observations of 3C 120 and compare these with previous observations obtained 1 yr previously.

2. OBSERVATIONS AND DATA ANALYSIS

The 86 GHz CMVA observation took place on 1997 October 24 (epoch 1997.82). Participating antennas were Pico Veleta, Effelsberg, Onsala, Metsähovi, Haystack, Kitt Peak 12 m, and VLBA Pie Town. The data were correlated with the Haystack Mk III correlator, after which global fringe fitting was performed within the NRAO Astronomical Image Processing System (AIPS) software. Because of bad weather at some of the stations and the relatively low flux density exhibited by 3C 120 during the observations, a significant amount of data were lost. We found a very consistent calibration for the American subarray of antennas, which was used to calibrate the rest.

The 7 mm and 1.3 cm VLBA observations were performed on 1997 November 10, 17 days apart from the CMVA observation. The data were recorded in 1 bit sampling VLBA format with 32 MHz bandwidth per circular polarization. The reduction of the data was performed with the AIPS software in the usual manner (e.g., Leppänen, Zensus, & Diamond 1995).

[1] The National Radio Astronomy Observatory is a facility of the National Science Foundation operated under cooperative agreement by Associated Universities, Inc.

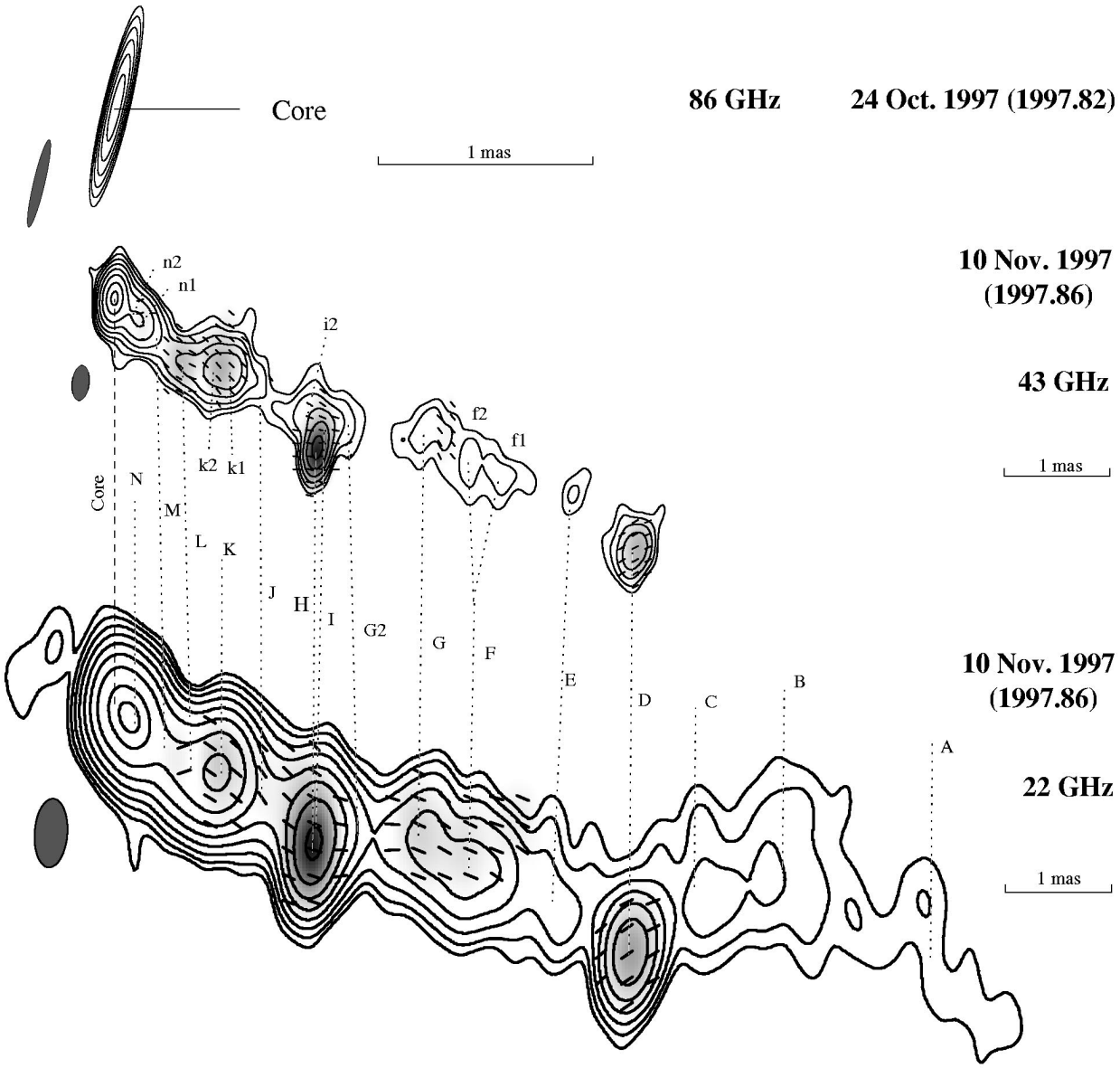

FIG. 1.—VLBI images of 3C 120 at 86 (*top*), 43 (*middle*), and 22 GHz (*bottom*). Total intensity is plotted as contour maps, while the linear gray scale shows the linearly polarized intensity (22 and 43 GHz only). The superposed bars give the direction of the *magnetic field* vector. For the 86, 43, and 22 GHz images, contour levels are in factors of 2, starting at (noise level) 2%, 0.9%, and 0.5% of the peak intensity of 1.51, 0.54, and 0.48 Jy beam^{-1}, respectively (43 and 86 GHz images contain an extra contour at 90% of the peak). Convolving beams (shown to the lower left of the core of each image) are 0.40 × 0.054, 0.32 × 0.16, and 0.63 × 0.30 mas, with position angles of −13°, −6°, and −4°. Peaks in polarized intensity are 27 and 42 mJy beam^{-1}, with noise levels of 3 and 2 mJy beam^{-1} for the 43 and 22 GHz images, respectively. The epoch and scale of each map are shown on the right (note that 86 GHz map scale is twice that of the other maps).

Opacity corrections were introduced by solving for receiver temperature and zenith opacity at each antenna. Fringe fitting to determine the residual delays and fringe rates was performed for both parallel hands independently and referred to a common reference antenna. Delay differences between the right- and left-handed polarization systems were estimated over a short scan of cross-polarized data of a strong calibrator (3C 454.3). The instrumental polarization was determined by using the feed solution algorithm developed by Leppänen et al. (1995).

The absolute phase offset between right- and left-circular polarization at the reference antenna was determined by VLA observations of the sources 0420−014 and OJ 287 on 1997 November 21 and referenced to an assumed polarization position angle of 33° for 3C 286 and 11° for 3C 138, at both observing frequencies. This provided an estimation of the absolute polarization position angle within 9° and 7° at 22 and 43 GHz, respectively.

3. RESULTS AND CONCLUSIONS

Figure 1 shows the resulting CMVA and VLBA images of 3C 120. Table 1 summarizes the physical parameters obtained for 3C 120 at the three frequencies. Tabulated data correspond to total flux density (S), polarized flux density (P), magnetic vector position angle (χ_B), separation (r), and structural position angle (θ) relative to the easternmost bright component (which we refer to as the "core") and angular size (FWHM). Components in the total intensity images were analyzed by model

TABLE 1
PHYSICAL PARAMETERS OF 3C 120

COMPONENTS 13 mm (7 mm)	S (mJy)		P (mJy)		χ_B (deg)		r (mas)		θ (deg)		FWHM (mas)	
	13 mm	7 mm	13 mm	7 mm	13 mm	7 mm	13 mm	7 mm	13 mm	7 mm	13 mm	7 mm
Core[a]	324	551	...	...	...	...	...	...	...	...	0.11	0.04
N (n2, n1)	374	109, 144	...	..., 5	...	..., 100	0.27	0.21, 0.34	−132.4	−130.2, −131.3	<0.01	0.01, 0.06
M (m)	129	50	4	...	113	...	0.61	0.52	−131.9	−130.3	<0.01	0.10
L (l)	205	71	...	14	...	59	0.95	0.84	−130.7	−133.1	0.19	0.16
K (k2, k1)	398	193, 173	12	21[b]	55	43[b]	1.17	1.11, 1.28	−122.6	−125.6, −122.0	0.20	0.22, 0.15
J (j)	64	25	4	4	34	34	1.60	1.58	−121.6	−121.5	0.22	0.14
I (i, i2)	257	37, 92	50[c]	33[d]	69[c]	70[d]	2.17	2.29, 2.09	−120.9	−122.0, −120.7	0.31	0.05, 0.31
H (h)	213	183	50[c]	33[d]	69[c]	80[d]	2.28	2.33	−127.2	−126.8	<0.01	0.02
G2 (g2)	15	26	...	...	...	...	2.53	2.44	−118.2	−119.2	0.16	0.17
G (g)	96	58	13	8	65	41	3.07	3.12	−113.8	−113.4	0.40	0.38
F (f2, f1)	117	30, 40	11[e]	..., 4	64[e]	..., 47	3.64	3.60, 3.94	−114.7	−114.2, −114.8	0.48	0.24, 0.35
E (e)	38	14	...	...	...	...	4.42	4.60	−114.1	−113.7	0.50	0.14
D (d)	156	124	23	15	125	118	5.26	5.32	−115.7	−115.8	0.15	0.17
C (...)	45	...	...	...	...	...	5.59	...	−108.3	...	0.76	...
B (...)	52	...	...	...	...	...	6.34	...	−104.0	...	0.93	...
A (...)	29	...	...	...	...	...	7.90	...	−107.3	...	1.19	...

[a] CMVA 3 mm observations reveal a total flux density of 1.51 Jy. Pico Veleta obtained an integrated total flux density of 1.95 ± 0.05 Jy (H. Ungerechts 1998, private communication).
[b] Common value for components k1 and k2, both blended in polarization.
[c] Common value for components I and H, both blended in polarization.
[d] Although components i and h appear blended in polarized flux, a slightly different χ_B can be observed.
[e] There is some extension in polarization northwest of F with a flux density of 8 mJy and $\chi = 93°$.

fitting the *u-v* data with circular Gaussian components within the software DIFMAP (Shepherd 1997). We have obtained an estimation of the errors in the model fitting by introducing small changes in the fitted parameters and studying the variations in the χ^2 of the fit as well as reproducing the model fitting from the start and comparing with previous results. For the 43 GHz image, the estimated model fitting errors are of the order of 5 mJy in flux, between 0.01 and 0.02 mas in position, and ~0.01 in component sizes. Larger errors, of the order of 50% higher, are estimated for the 22 GHz image model fitting.

The 3 mm CMVA image of Figure 1 shows the existence of a bright core component. The mapping process was able to recover 1.51 Jy of the integrated total flux of 1.95 ± 0.05 Jy measured by Pico Veleta (H. Ungerechts 1998, private communication), resulting in a maximum brightness temperature of 1.15×10^{10} K. The combined spectrum for the core at the three observing frequencies gives an inverted spectrum with $\alpha \sim 1.1$ ($S_\nu \propto \nu^\alpha$). Components n1 and n2 show a steep spectrum between 22 and 43 GHz, which, together with the inverted spectrum of the core, would explain why they are not detected in the 86 GHz map, given the relatively poor dynamic range of the latter. Metsähovi flux density monitoring at 22 and 37 GHz (H. Teräsranta 1998, private communication) observed the strongest radio flare ever seen in 3C 120 to take place starting at the end of 1997 and peaking in 1998 June, which would explain the flattening of the spectrum of the core with respect to the late 1996 observations. No polarization was detected for the core at either 22 or 43 GHz.

We estimate the size of the core to lie below the resolution of the 86 GHz map, that is ≤54 μas, which implies a linear size less than 0.025 h^{-1} pc, or 30 lt-days. This represents a direct determination of the upper limit to the size of the base of the jet that is independent of variability arguments, which depend on the quite uncertain estimate of the Doppler factor.

The 43 and 22 GHz images show a much richer structure consisting of multiple components. We have labeled components from west to east, using uppercase letters for the map at 22 GHz. We shall note that several of the components in the 43 GHz image appear blended in the corresponding 22 GHz image. Through comparison with previous images obtained at the end of 1996 (G98) and extrapolation of the component speeds, we have cross-identified several components. The most reliable identification corresponds to components A, B, C, and D. Components H and K may be associated with two distinct radio flares detected by Metsähovi (H. Teräsranta 1998, private communication) at the end of 1996 and in mid-1997, with component H appearing previously in the 1996 November and 1996 December images of G98.

In comparison with the late 1996 epochs of G98, components A, B, C, E, F, and G are found to have experienced a similar evolution. Each moved along the curved path traced by the jet in the plane of the sky. During this downstream translation, their flux densities declined at both observing frequencies (except for component E at 43 GHz). This is as expected for components that are subject to expansion and radiative cooling (the latter of which might have occurred earlier and become prominent at radio frequencies only after further expansion). There is some evidence for deceleration of components upstream of D to a common value close to ~3 $h^{-1}c$, but further observations are needed to confirm this. One of the largest variations can be found in polarization. Components F and G decreased their polarized flux density between 1996 November and December to undetectable values, but by 1997 November showed an increase to values between 9% and 14%. This change was accompanied by a rotation of the magnetic field vector from orthogonal to parallel to the jet axis. Components B and C experienced a similar drastic variation, changing their degree of polarization from values close to 10% in late 1996 to values below the noise in the images in Figure 1. This suggests changes in the underlying configuration of the magnetic field and/or the shocks presumably associated with the components in the inner parsec of 3C 120.

We found a significantly different evolution for component D. During the 1 yr period between the G98 observations and that shown in Figure 1, component D gained flux and its spectrum became significantly flatter. Even more pronounced

changes are found in polarization, from below the noise level in the G98 observations to a level that made it one of the strongest components in polarized flux density, with a degree of polarization of 15% (13% at 43 GHz). All this evidence suggests significant activity in component D not present in the other components.

We interpret the different evolution occurring in component D as being caused by its interaction with the external medium. As shown in the 22 GHz image, the jet clearly bends at the position of D, so we expect at least a standing oblique shock there. While between late 1996 and 1997 November the position angle of components B and C rotated by ~3°, the increment in component D was significantly smaller, of the order of 1.°5. As a consequence, the curvature near component D appears more pronounced than in the previous images of G98, actually showing component D centered ~0.3 mas south of the jet axis defined by components E and C. If the jet components travel along a gently curved jet funnel, it is possible that components with relatively larger momentum—as may be the case for D—would move along a more ballistic trajectory, progressively moving closer to the jet funnel boundary and consequently undergoing interactions with the external medium. This would explain the more ballistic trajectory of component D, while other components seem to have followed the curvature of the jet. The interaction with the external medium should produce a strong shock and turbulence (from Rayleigh-Taylor and perhaps Kelvin-Helmholtz instabilities), enhancing the emission and flattening the spectrum, as is commonly observed in the terminal hot spot of large-scale jets. The shock would also produce an enhancement and reordering of the magnetic field parallel to the shock front; this would explain the increase in the polarized flux and degree of polarization. The magnetic field orientation in D is consistent with this scenario and contrasts with that observed for the rest of the jet, which is roughly parallel to the jet flow (except for components n1 and M).

Component H seems to share some of the properties and activity of component D. Its structural position angle shifted to the south by 2.°5, which placed it ~0.25 mas south of the jet axis in 1997 November. The spectrum is flatter at this later epoch, and the degree of polarization increased from values below 4% at the end of 1996 to 23% (18% at 43 GHz) in 1997 November, the maximum value measured in the jet. During this burst in polarization, H maintained a similar orientation of its magnetic field, almost parallel to the jet axis, with a slightly shifted orientation at 43 GHz toward the direction of component d's field. To the north of H (h at 43 GHz), model fitting reveals the presence of component I (i), which presumably is traveling through the jet funnel out of which H seems to be breaking. This is suggested by a slightly different orientation of the magnetic field position angle.

The structural position angle of the inner milliarcsecond components in 3C 120 underwent a mean shift to the south of ~6° between late 1996 and 1997. This indicates a progressive swing of the jet ejection direction toward the south, which may be responsible for the continuous curvature observed on parsec and kiloparsec scales (e.g., Walker 1997). It is then expected that some components (perhaps with relatively larger momentum)—such as D and H—would experience strong interactions with the external medium, opening a new path through which subsequently ejected components would travel relatively undisturbed.

Further observations (in progress) will provide a follow-up of the changes observed in 3C 120 and test the hypothesis presented here as well as allow comparison with simulations of the hydrodynamics and emission of relativistic jets (Gómez et al. 1997), resulting in a better understanding of the physics involved in 3C 120 and other active galactic nuclei.

This research was supported in part by Spain's Dirección General de investigación Científica y Técnica (DGICYT) grants PB94-1275 and PB97-1164, by NATO travel grant SA.5-2-03 (CRG/961228), and by US NSF grant AST 98-02941. We thank Iván Agudo-Rodríguez for preparing Figure 1. We thank Robert Phillips and Elisabeth Ambrose for providing confirmation of the CMVA results through a map obtained using the software HOPS. We are also grateful to Barry Clark for providing ad hoc VLA time in order to determine the absolute polarization position angle.

REFERENCES

Benson, J. M., Walker, R. C., Unwin, S. C., Muxlow, T. W. B., Wilkinson, P. N., Booth, R. S., Pilbratt, G., & Simon, R. S. 1988, ApJ, 334, 560
Burbidge, E. M. 1967, ApJ, 149, L51
Gómez, J. L., Marscher, A. P., Alberdi, A., Martí, J. M., & Ibáñez, J. M. 1998, ApJ, 499, 221
Gómez, J. L., Martí, J. M., Marscher, A. P., Ibáñez, J. M., & Alberdi, A. 1997, ApJ, 482, L33
Hjorth, J., Vestergaard, M., Sorensen, A. N., & Grundahl, F. 1995, ApJ, 452, L17
Leppänen, K. J., Zensus, J. A., & Diamond, P. J. 1995, AJ, 110, 2479
Seielstad, G. A., Cohen, M. H., Linfield, R. P., Moffet, A. T., Romney, J. D., Schilizzi, R. T., & Shaffer, D. B. 1979, ApJ, 229, 53
Shepherd, M. C. 1997, in ASP Conf. Ser. 125, Astronomical Data Analysis Software and Systems VI, ed. G. P. Hunt & H. Edward (San Francisco: ASP), 77
Walker, R. C. 1997, ApJ, 488, 675
Walker, R. C., Benson, J. M., & Unwin, S. C. 1987, ApJ, 316, 546